The Influence of the Cathode Tip on Temperature and Velocity Fields in a Gas-Tungsten Arc

Maintenance of a sharp cathode tip offers the possibility of more uniform quality of the weldments produced with a gas-tungsten arc.

BY T. W. PETRIE AND E. PFENDER

ABSTRACT. To find the influence of the sharpness of the cathode tip on temperature and velocity fields in a gas-tungsten arc, a free-burning arc in argon at atmospheric pressure is studied. Detailed measurements of the temperature and velocity fields are presented for a sharply-pointed, thoriated tungsten cathode. With this sharp tip, the arc is severely constricted at the cathode.

Data are also gathered after loss of the sharply pointed tip. Comparison to these data and also to results obtained with free-burning arcs having blunt cathodes shows that the sharpness of the cathode tip has little effect on the temperature field. However, the effect on the velocity field is marked. The severe constriction leads to as much as a 50% increase in the velocity. It may also increase the peak current density to the anode by the same amount. Both effects cause the heat flux distribution at the anode to become narrower and to have a higher peak value.

In applications of the gas-tungsten arc, the maintenance of a sharply pointed cathode is expected to increase the penetration and to decrease the width of the area of the workpiece affected by the arc

Introduction

In gas tungsten-arc welding, the heat flux distribution on the workpiece or arc anode is strongly influenced by the temperature and velocity fields in the arc. These fields, in turn, depend on the shape of the tip of the non-consumable cathode. If, for example, the tip is sharply pointed, then the arc is highly constricted at the cathode, resulting in narrow peaks in the temperature and velocity fields. On the other hand, a blunt cathode tip allows a more diffuse arc attachment at the cathode and less severe peaks in the fields. Within certain limits, therefore, the flow and temperature fields may be controlled by the cathode shape.

To investigate the influence of the cathode tip on temperature and velocity fields, a high-intensity, free-burning arc is employed. It discharges between a thoriated tungsten cathode and a flat, watercooled copper anode in argon at atmospheric pressure. The arc region is rotationally symmetric about the centerline of the cathode and the anode is perpendicular to the cathode. This arc is similar to a gas-tungsten arc, except for cooling and positioning of the anode. However, the cathode configuration of both arcs is the same so that the effect of cathode shape obtained with a free-burning arc is applicable to actual welding arcs. The particular free-burning arc used in this study allows long-time operation of an arc in a fixed position and generates a rotationally symmetric plasma. These features permit measurement of the temperature and velocity fields with established techniques.

Measurement of the temperature field is accomplished by spectrometric techniques. The applicability of spectrometric techniques has been documented for high-intensity arc plasmas and, in particular, for free-burning arc configurations.[1] The resulting temperatures are considered accurate to within ±5%.[2] Of various methods available to determine the temperature spectrometrically, the absolute line intensity, the ion-neutral line ratio, the off-axis peaking, and the continuum intensity methods are selected to yield a consistent and accurate mapping of the temperature field. Furthermore, the temperatures measured in this study are directly comparable to the results of a previous study.[3]

The velocity field results from the cathode jet of the free-burning arc. This jet arises from the balance of pressure and Lorentz forces acting on the charged particles in the plasma.[4] Through collisions between the charged and neutral particles, a high velocity flow of al plasma constituents is directed downstream from the cathode in the axial direction.

Wienecke[5] photographed a free-burning, high-intensity carbon arc in air to measure the cathode jet velocity. He disconnected the power to the arc and re-established it electronically a very short time later. The series of pictures taken at brief time intervals after reignition shows the development of the cathode jet. Because they are obtained during arc start-up, it is doubtful whether the values of velocity obtained by comparison of successive pictures are the same as the velocities which are obtained in the steady state. Nevertheless, those measurements indicate the order of magnitude of the jet velocities to be expected in such high intensity arcs.

Kimura and Kanzawa[6] insert a small metal plate in a free-burning arc with tungsten cathode in argon and record the drag force on this plate using a pressure transducer. Independent temperature measurements are also made. The drag plate is calibrated by measuring its drag coefficient as a function of Reynolds number. The error involved in the resulting velocities is estimated at less than 17.5%. However, excluded from this estimate is the effect which insertion of the drag plate has on the arc discharge and, subsequently, on the velocity field. This effect is neglected on the basis of motion picture records of the arc appearance during the insertion of the drag plate.

A third method of measuring the velocity of the cathode jet is due to Schoeck.[7] It is an application of pressure probes to plasma. The anode is used as a combination electrode and pressure probe by drilling a hole in it and monitoring the pressure on the anode face with a manometer. Given this pressure, boundary layer theory allows the calculation of the velocity of the oncoming

T. W. PETRIE is an Assistant Professor of Mechanical Engineering at the University of Illinois at Urbana-Campaign, Urbana, Illinois and E. PFENDER is a Professor of Mechanical Engineering at the University of Minnesota, Minneapolis, Minn.

flow. Since this method allows the arc to definitely be in steady state, it is the method adopted here for direct measurement of the velocity along the arc axis. Values off the arc axis are computed from a numerical integration of the momentum equation for plasmas[4] and are normalized to the measured values on the axis.

By applying these measurement techniques, a complete profile of the temperature and velocity fields throughout the arc region can be generated. Complete results are presented for a sharply pointed cathode. The influence of the cathode tip on the temperature and velocity fields is presented by comparing results for other cathode tip conditions to the results with a sharply pointed tip. In this way, it is hoped that guidelines will be establsihed to judge the acceptability of various cathode tip conditions in particular applications of gas-tungsten arcs.

Experimental Apparatus

The free-burning arc used in the experiments requires approximately 4kw of direct current power. This is provided with less than 0.5% ripple by the 200 kw rectifier of the High Temperature Laboratory in the Mechanical Engineering Dept. of the University of Minnesota. A high frequency arc starter is used to facilitate initial breakdown of the arc gap. Provisions are made for continuous monitoring of the arc voltage and current. A manual adjustment of the arc current is available through a potentiometer on the rectifier control panel.

To ensure carefully controlled atmospheric conditions for operation of the free-burning arc, a special arc chamber is included in the experimental apparatus. Shown in Fig. 1, this chamber is constructed of stainless steel. It is leak-free to the detection limit of a mass spectrometer type, helium-sensitive leak detector and is evacuated to 10^{-6} Torr before being filled from cylinders of 99.995% pure argon. To further remove impurities, especially oxygen and water vapor, the argon is passed through a tube filled with heated titanium chips before being admitted to the chamber. During the temperature and velocity measurements included in this study, the forkshaped probe holder was not part of the chamber.

All surfaces of the chamber exposed to the arc are water-cooled to ensure structural integrity and to allow steady-state arc operation. The cathode can be moved vertically to adjust the arc gap and the entire cathode assembly is movable in the plane perpendicular to the cathode axis to permit precise alignment of the cathode tip with respect to the center of the anode.

The latter adjustment is made necessary by the combination anode and pressure probe used in the velocity measurement and shown in Fig. 2. For comparison, Fig. 2 also shows a view of the regular anode already shown in the arc chamber in Fig. 1. The main feature of the pressure-tapped anode is the small hole in its face. This hole is precisely aligned with respect to the arc axis by placing a special cap over the cathode tip. This cap has the smooth end of the drill bit used to form the hole in the anode imbedded in the side facing the

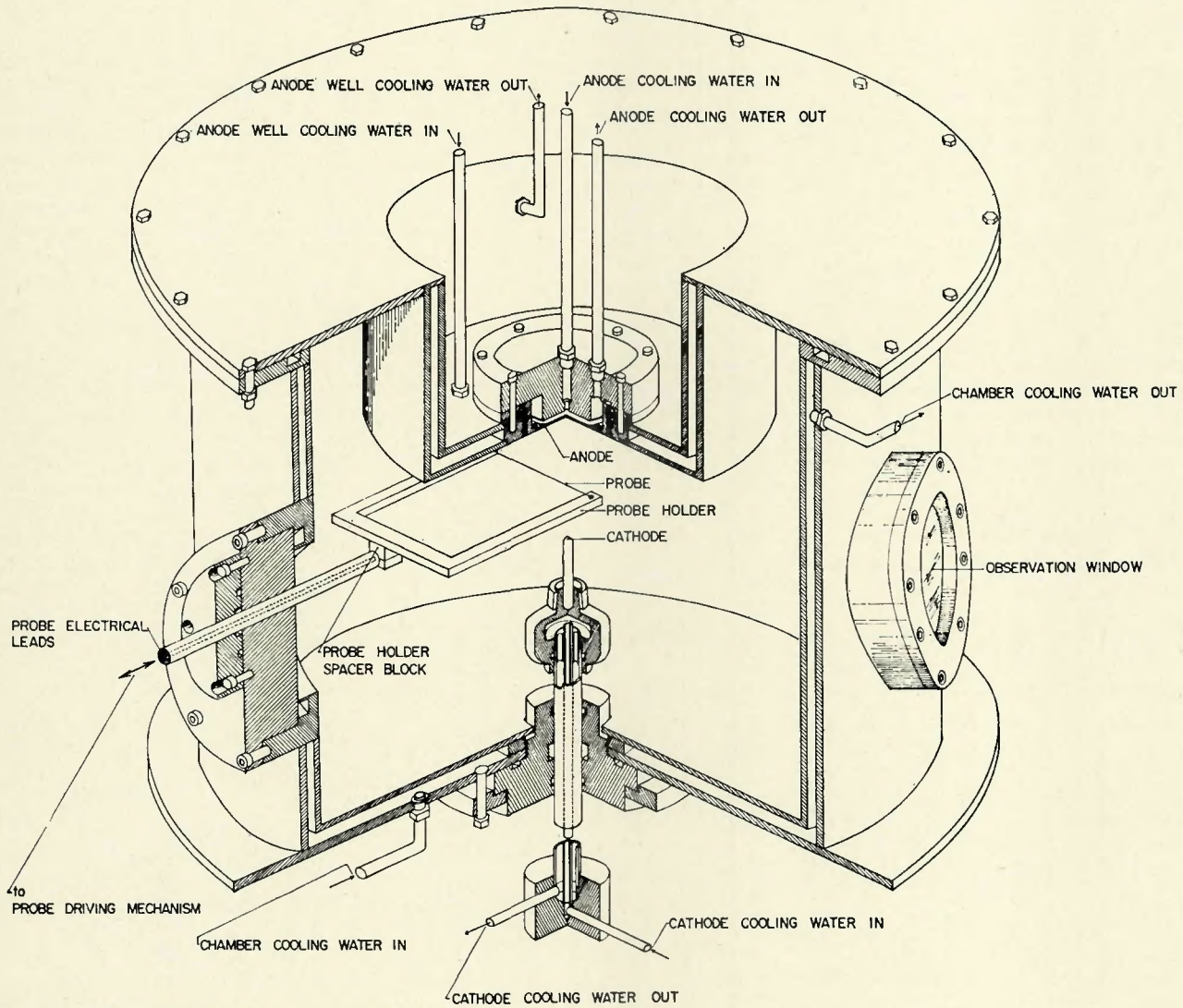

Fig. 1—Schematic diagram of arc chamber

anode. When the cathode is properly aligned and the arc gap is decreased, this pin fits into the hole in the anode. Because of the difficulty of placing the hole in the anode in any position except directly over the cathode tip, only velocity measurements on the arc axis can be made with this pressure-tapped anode.

Both the regular and the pressure-tapped anode are made of copper and are water-cooled on their back faces. A set of cathodes are made of pieces of 2% thoriated tungsten rod, ¼ in. in diameter and approximately 3 in. long. These rods are sharpened at one end and are inserted into the water-cooled cathode holder.

It is not possible to make all the desired temperature and velocity measurements in a short time. The results included in this paper are from many different experiments run during a span of several months. In order to begin each experiment with the same arc conditions, therefore, a standard operating procedure was devised and strictly followed. As has been mentioned, part of this procedure included evacuation of the arc chamber before each experiment to 10^{-6} Torr and slowly filling it with specially cleaned argon.

An equally important part of this operating procedure concerns the preparation of the electrodes. During an experiment and owing to the action of the cathode jet, minute quantities of tungsten are deposited on the anode. To prevent build-up of this deposit, the anode is polished with a fine abrasive and is cleaned with acetone before each experiment. In addition, the cathode tip is watched closely for signs of deterioration. Figure 3 is a photograph of three cathodes showing typical conditions of the cathode tip. Before an experiment, a polished cathode is installed with a sharply pointed tip as shown on the right of Fig. 3. Machining of the tip is accomplished in a lathe using a carbide tool bit. In the middle of the picture is a cathode as it appears after approximately one-half hour of arc operation. The cathode tip is still intact, constricting the arc to attachment at this point.

In the left of Fig. 3, a cathode is shown after prolonged arc operation. Note the loss of the sharp tip which is accompanied during arc operation by a noticeable change in the severity of the arc constriction at the cathode. In the free-burning arc used in this study, the tip was propelled to the anode and became lodged there in some random position with respect to the center of the anode. This sometimes caused a preferred arc attachment spot at the anode and loss of rotational symmetry of the arc. Rotational symmetry is demanded by the spectrometric techniques used to measure the plasma temperature. At other times, no severe loss of symmetry was apparent, although the arc attachment spot at the cathode had a tendency to wander around on the blunted cathode. The results presented in this paper and identified as being obtained after the loss of the cathode tip are for the case when symmetry is retained.

Measurement of the Temperature Distribution

Attention throughout this study is focused upon a free-burning arc in argon at atmospheric pressure. The arc gap is held constant at 10 mm and the arc current is kept at 200 amp. These values of arc parameters are chosen to permit direct comparison with the temperature distribution obtained in this laboratory by Wutzke, et al.[3] Furthermore, the arc current of 200 amp and the atmospheric pressure ensure that deviations from local thermodynamic equilibrium (LTE) in the engineering sense* are confined to distances less than a fraction of a millimeter from the cathode tip.[2]

* Strictly speaking, the existence of partial LTE only is postulated, which is less restricted than complete LTE. Partial LTE, in contrast to complete LTE, does not require that the population of lower-lying energy levels of atoms and ions, especially of the ground state particles, follow the same Boltzmann distribution as the upper levels. This effect is immaterial in many engineering applications in which enthalpies, internal energies, etc., are of interest. For spectrometric measurements, however, deviations from a complete LTE population of excited states become important as soon as transitions from lower levels are considered. The spectrometric methods applied in this study consider transitions from upper levels and from the electron continuum only.

The spectrometric techniques applied to measure the plasma temperatures involve measuring the intensity of radiation emitted at certain wavelengths from the plasma. The plasma is assumed to be optically thin. The radiation intensity at a given wavelength is calculated from an elemental volume of plasma in LTE at various temperatures. The temperature of the plasma element of interest is obtained by comparing the calculated and measured intensities of radiation.

In the case of a free-burning arc, it is impossible to measure the radiation from an isothermal element of plasma. Instead, a narrow beam of the plasma is viewed from the side in planes perpendicular to the cathode and at various distances from the cathode tip. This so-called lateral intensity of radiation is recorded at various wavelengths as the spectrometer scanning system is swept across a given plane from the plasma fringe through the arc axis to the opposite fringe.

The plasma is assumed rotationally symmetric about the arc axis. This assumption is justified by Fig. 4. The symbols represent lateral intensities of radiation from a sweep across the free-burning arc with a sharply pointed cathode. The solid curves shown are symmetrical, being formed by folding a plot of the data about the axis. No significant deviation of the data from the curves is apparent in this typical display of lateral intensities.

For a rotationally symmetric, optically-thin plasma, the lateral intensity of radiation is converted to radial emission coefficients using the Abel inversion equation:[8]

$$\epsilon(r) = -\frac{1}{\pi}\int_r^R \frac{I'(x)\,dx}{\sqrt{x^2 - r^2}} \qquad (1)$$

where $\epsilon(r)$ is the local emission coefficient and $I'(x)$ is the first derivative of the measured lateral radiation intensity. In planes perpendicular to the arc axis, R is the radius of the arc from axis to fringe, r is an arbitrary radial distance from the arc axis in the range zero to R, while x is the distance to the axis from the center of the chord for which the lateral intensity is being measured. The

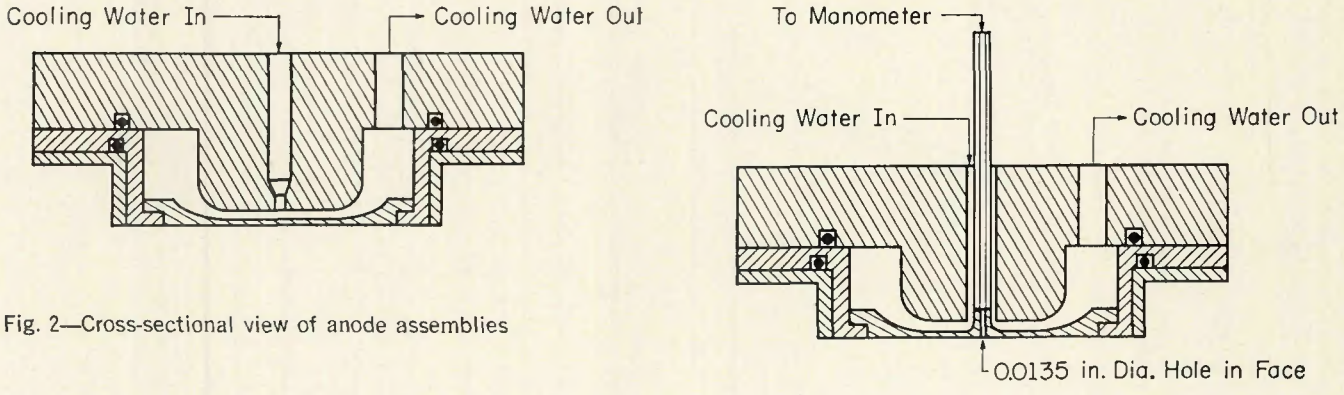

Fig. 2—Cross-sectional view of anode assemblies

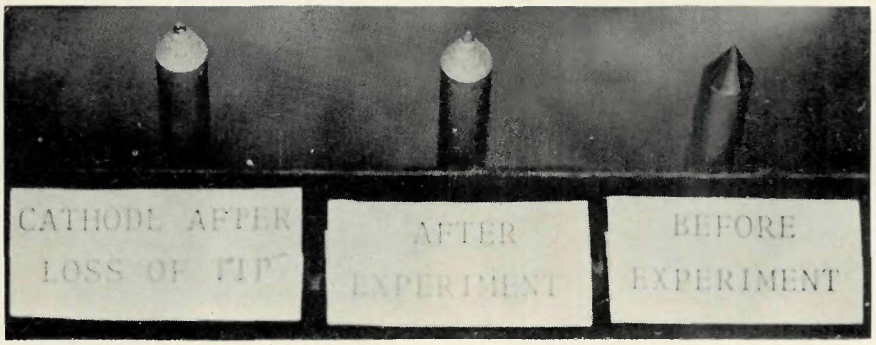

Fig. 3—Effect of arc operation on pointed cathodes

radial emission coefficients from eq (1) are values of radiation emitted from an element of plasma and yield the desired local values of the plasma temperature when compared to calculated emission coefficients. The Abel inversion and the comparison to calculated emission coefficients are performed on a digital computer.

The reduction of the lateral intensities at the various wavelengths to yield the desired plasma temperatures is done with four methods: the absolute line intensity, the ion-neutral line ratio, the off-axis peaking, and the continuum intensity methods. The first three methods utilize the fact that the radiation emitted at a given wavelength is the result of a transition from an energy state χ_s to a lower state χ_t. The frequency of the emitted photons is given by the Bohr frequency relation:

$$\chi_s - \chi_t = h\upsilon \qquad (2)$$

where h is Planck's constant and υ is the frequency at which the radiation is observed. In general, the line emission coefficient for radiation emitted at frequency υ from an optically thin homogeneous plasma is expressed by:

$$\epsilon_L = \frac{1}{4\pi} A_{r,\,t}{}^{r,\,s}\, n_{r,\,s}\, h\upsilon \qquad (3)$$

where ϵ_L is the line emission coefficient and $A_{r,\,t}{}^{r,\,s}$ is the transition probability for the spontaneous transition of an r-times ionized atom from a quantum level s to a lower level t. The values of those needed for this study are available in the literature. The quantity $n^{r,\,s}$ is the number density of r-times ionized atoms in the sth quantum state. This number density may be expressed by a Boltzmann distribution if LTE prevails in the element of plasma; viz.,

$$n_{r,s} = n_r \frac{g_{r,s}}{Z_r} \exp(-\chi_{r,s}/kT) \qquad (4)$$

where n_r is the total number density of r-times ionized atoms, $g_{r,s}$ is the degeneracy of the sth quantum level of this species, Z_r is its partition function, $\chi_{r,s}$ is the energy of the sth quantum level of this species, k is the Boltzmann constant, and T is the temperature at which the plasma element, including the $n_{r,s}$ atoms, is radiating.

The line emission coefficient ϵ_L is an integrated value over the natural width Δx of a spectral line. It refers to emission from an optically thin, homogeneous slab of unity thickness, From eqs (3) and (4), one obtains:

$$\epsilon_L = \frac{1}{4\pi} A_{r,t}{}^{r,s} n_r \frac{g_{r,s}}{Z_r} \exp(-\chi_{r,s}/kT)\, h\upsilon \qquad (5)$$

The line emission coefficient for a particular line depends, therefore, only on the temperature. This dependence appears explicitly in the exponential term and implicitly in the number density n_r. The partition function Z_r is also a function of temperature, although weakly so. The line emission coefficient is a function of the radius in a plane perpendicular to the axis of a rotationally symmetric plasma and can be obtained experimentally from the solution of eq (1) for the local emission coefficients. The desired plasma temperatures obtained from eq (5) are also functions only of the radius in these planes.

If the absolute value of the line emission coefficient is available, then eq (5) directly yields the plasma temperature. This is the basis of the absolute line intensity method used here. However, calibration of the optical system is required. In this study, a standard carbon arc acts as the radiation source for calibration.

The ion-neutral line ratio method does not require this calibration. Considering the intensity ratio of spectral lines produced by transitions in neutral (subscript 0) and singly ionized species (subscript +), eq (5) yields:

$$\frac{\epsilon_{L+}(T)}{\epsilon_{L0}(T)} = \frac{n_+ Z_0 (A_t{}^s g_s \upsilon)_+}{n_0 Z_+ (A_t{}^s g_s \upsilon)_0} \exp\left(\frac{\chi^{s,0} - \chi^{s+}}{kT}\right) \qquad (6)$$

The only requirement imposed on the spectrometer in using this method is that it measure ϵ_{L+} and ϵ_{L0} on the same relative scale. The large difference in energy between the neutral and singly ionized states, $\chi_{s0} - \chi_{s+}$, makes the ion-neutral line ratio method more accurate than line ratio methods using

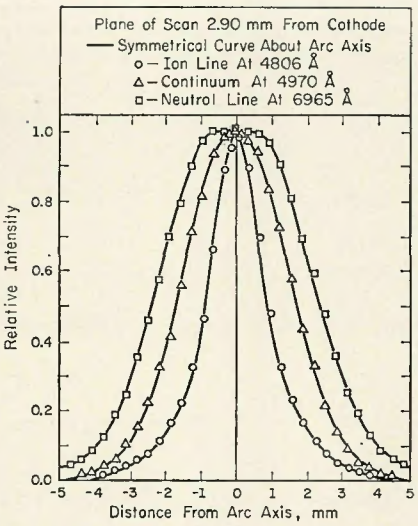

Fig. 4—Symmetry of the free-burning arc with a sharply pointed cathode

two lines from the same stage of ionization.

The off-axis peaking method takes advantage of the fact that the line emission coefficient given by eq (5) has a maximum for a temperature T^*. This is due to the interaction of the increasing exponential and the decreasing number density n_r as temperature increases at constant pressure. The latter decreases not only because of the perfect gas law, but also because of loss of r-times ionized particles by ionization to $r+1$-times ionized states. In argon at atmospheric pressure, neutral lines exhibit this maximum in ϵ_L at approximately 15,500° K. The ratio of neutral line emission coefficients at a temperature T and T^* is, again from eq (5):

$$\frac{\epsilon_L(T)}{\epsilon_L(T^*)} = \frac{n_0(T)\; Z_0(T^*)}{n_0(T^*)\, Z_0(T)} \exp\left[\frac{\chi_s}{k}\left(\frac{1}{T} - \frac{1}{T^*}\right)\right] \qquad (7)$$

No absolute calibration of the optical system is needed.

Unlike radiation from spectral lines, the radiation continuum is independent of the frequency for $\upsilon \leq \upsilon_g$ where υ_g is a break-off frequency characteristic of a particular continuum regime. For these continuum regions, according to Kramers-Unsöld theory, the absolute emission coefficient ϵ_υ at a convenient frequency υ is given by:

$$\epsilon_\upsilon = C Z_{eff}{}^2 \frac{n_e n_i}{\sqrt{kT}} \qquad (8)$$

where C is a constant, Z_{eff} is the effective average charge on the ions, n_e is the electron density, and n_i is the ion density. Continuum radiation in a plasma arises from the interaction of electrons and ions. Z_{eff} is not necessarily the same as the ionic charge owing to the fact that fast electrons may penetrate the outer electron shells of ions with

Table 1—Relative Peak Lateral Intensity of Radiation at Various Wavelengths as a Function of Time of Arc Operation

	1.55 mm from cathode tip			2.90 mm from cathode tip		
Sequence	4806 Å	4950 Å	6965 Å	4806 Å	4950 Å	6965 Å
First	1.00	1.00	1.00	0.97	1.00	—
Second	0.76	0.99	—	1.00	0.92	1.00
Third	0.71	0.95	—	0.75	0.97	1.00
Fourth	0.54	0.83	0.92	0.67	0.95	—

	4.05 mm from cathode tip			5.40 mm from cathode tip		
Sequence	4806 Å	4950 Å	6965 Å	4806 Å	4950 Å	6965 Å
First	1.00	1.00	—	1.00	1.00	1.00
Second	0.91	0.87	1.00	0.96	0.96	—
Third	0.79	0.97	0.98	0.75	0.84	—
Fourth	0.81	0.95	—	0.78	0.90	0.92

many shells and, in effect, see a higher ionic charge. In applying eq (8), the factor CZ_{eff}^2 is modified to yield adequate agreement over the range of data from experiment.[1]

In the argon spectrum, numerous lines and continuum regimes are available to yield reliable plasma temperatures. An optically thin plasma is needed to observe all the radiation making up the lateral intensity at a given wavelength. Furthermore, in the case of spectral lines, accurate transition probabilities are needed to calculate the radial emission coefficients. Also, the source of radiation at a given wavelength must be known and the intensity must be sufficiently strong to detect against the background continuum and the electronic noise of the spectrometer.

In this study, radiation intensities from the ion line at 4806 Å, the neutral lines at 4300 and 6965 Å, and the continuum near 4950 A in the argon spectrum are recorded. The transition probability of Olsen[9] at 4806 Å is used. For the neutral lines, data are taken from Coates and Gaydon[10]. Measurements in this study at 4300 Å are unreliable, expecially near the cathode, owing to the proximity to 4300 Å of a line of the tungsten spectrum. The severe constriction of the arc at the cathode caused by the use of a sharply pointed cathode leads to evaporation of cathode material so that traces of tungsten are present in the arc. The most reliable data are obtained at 6965 Å. Corrections for self-absorption, that is, lack of an optically thin plasma, are, in general, necessary at 6965 Å. However, for temperature measurements, these corrections are considered superfluous, involving at most an improvement of 3% in the accuracy of the temperature obtained.[11]

The lateral intensities of radiation are recorded for various planes perpendicular to the arc axis. In order to obtain a profile of a large portion of the arc plasma, the planes studies are 1.55, 2.90, 4.05, and 5.40 mm from the cathode tip of the 10 mm arc. In addition to obtaining reliable plasma temperatures, it is also desired to check the effect of cathode tip sharpness on the temperature field. From preliminary runs, it was noted that a sharpened cathode would retain its tip for ample time to obtain data at all the wavelengths of interest in any one plane, except 6965 Å. Approximately 20 min are required to scan one plane for these data. The data at 6965 Å require a different photomultiplier tube for detection of the radiation. Therefore, these data are obtained in separate runs. The cathode tip remained intact for at least the time needed for two planes in the 6965 Å runs.

The final data for all wavelengths except 6965 Å are gathered according to the following plan. In the first run, the plane 1.55 mm from the cathode tip is scanned initially. Then, in order, the 2.90, 4.05, and 5.40 mm planes are scanned. The second run begins with the 2.90 mm plane, followed by the 4.05, 5.40, and 1.55 mm planes in sequence. Run three with the 4.05 mm plane scanned initially and the fourth run with the 5.40 mm plane scanned initially complete this scheme. For the data at 6965 Å, a run with the 1.55, 2.90, 4.05, and 5.40 mm planes scanned in sequence and another run in the opposite order yield the desired results.

Table 1 presents the peak lateral intensity observed in each plane at 4806, 4950, and 6965 Å as a function of time of arc operation. The maximum intensity observed for each plane in the four time intervals and for each wavelength is given the value 1.00. The other intensities are given relative to this value.

As time of arc operation increases, the sharp tip of the cathode is first lost and then the remaining tip becomes more blunted. This decreases the constriction of the arc, making more area available to carry the same total current. Therefore, the average current density decreases in a given plane. Ohm's Law in the axial direction of the free-burning arc states that:

$$j_z(r) = \sigma(r) \cdot E_z(r) \qquad (9)$$

where j_z is the current density in the axial direction z, E_z is the applied electric field, and σ is the scalar electrical conductivity. Assuming as a rough estimate that the electric field in a given plane is uniform, an assumption used by Olsen in planes away from the cathode[2], then, as the average current density decreases, so must the average electrical conductivity. However, the electrical conductivity decreases monotonically with decreasing temperature for argon at atmospheric pressure[12]. This implies that the average plasma temperature decreases in a plane as the cathode tip becomes more blunt. The average temperatures of interest are below the temperature at which the emission coefficients reach a maximum. Therefore, the lateral intensity of radiation also decreases monotonically with decreasing temperature. Hence, the peak lateral intensity at a given wavelength should decrease as the cathode tip deteriorates. The behavior of the data in Table 1 corroborates this conclusion.

The lateral intensities of radiation from experiments in which the cathode tip remain intact are prepared for analysis by the absolute line intensity, ion-neutral line ratio, off-axis peaking, and continuum intensity methods. At least two of the four methods yield reliable results at each location in the planes of interest. The results are averaged to provide the temperature profiles in each plane. The maximum deviation from this average is $\pm 3\%$ in all plasma regions, except near the axis in the plane 1.55 mm from the cathode tip. The severe constriction due to the sharply pointed cathode causes equally severe gradients in the lateral intensity which increase the deviation to $\pm 6\%$.

The resulting temperature profiles are plotted to yield the isotherm map shown in Fig. 5. A direct comparison is made to the results obtained previously in this laboratory by Wutzke, et al.[3]. Their results are for an arc identical to the arc used in the study, except their data are average results obtained from long-time operation of the arc. Note that the con-

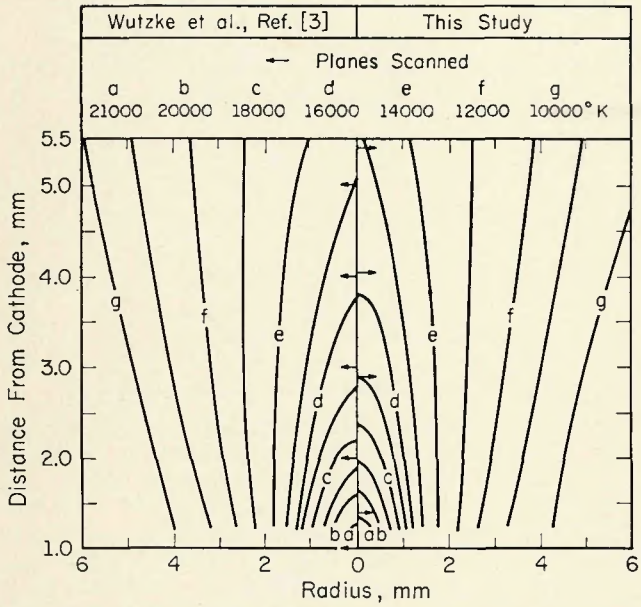

Fig. 5—Isotherms of the 200 amp, 10 mm free-burning arc in argon at atmospheric pressure

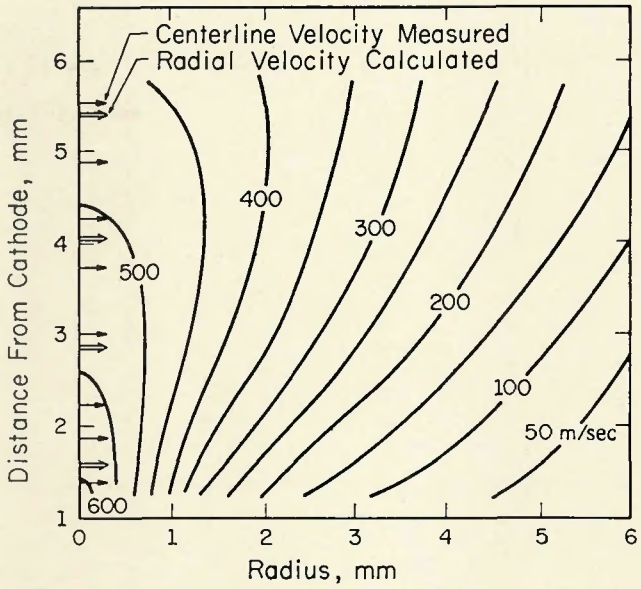

Fig. 6—Equal velocity curves of the 200 amp, 100 mm free-burning arc in argon at atmospheric pressure

clusion confirmed qualitatively by Table 1 concerning the effect of the cathode tip is confirmed quantitatively by Fig. 5. The effect of the sharply pointed cathode is to maintain a higher temperature in the arc core, while no appreciable difference is apparent in the location of the isotherms below 15,000° K. Moreover, higher temperatures are present further away from the cathode tip due to the stronger action of the cathode jet with a sharp cathode tip. The difference in the profiles is, however, not significantly different owing, it is speculated, to increased heat transfer outward from the arc core offsetting to a large extent the effects on plasma temperature of increased constriction with a sharp cathode tip.

Determination of the Flow Field

The flow field exerts a direct influence on the anode heat flux distribution by controlling the convection of heat to the anode. Indirectly, the flow field causes the free-burning arc to assume its characteristic bell shape. The radial extent of the plasma depends upon the constriction of the arc at the cathode and determines the current densities at the anode and the anode heat fluxes due to the electrical current. Therefore, the effect of cathode tip sharpness on the flow field in the free-burning arc is needed to fulfill the purpose of this study.

To measure the cathode jet velocity, an anode with a hole drilled in the center of its face is installed in the arc chamber in place of the regular anode. The hole in the pressure-tapped anode is aligned directly on the arc axis. The data obtained in an experiment with the pressure-tapped anode consist of the column heights of the liquid in a U-tube manometer for various distances of the anode from the cathode tip. One leg of the manometer is connected to the pressure tap in the anode and the other is exposed to the chamber pressure at a location outside the plasma. Thus, these experiments yield the stagnation pressure at the anode with respect to the static pressure in the arc chamber.

This pressure difference is related to the velocity of the approaching flow through the equation:

$$\Delta P_0 = \frac{1}{2}\rho_\delta U_\delta^2 \qquad (10)$$

where ΔP_0 is the measured pressure difference, while ρ_δ and U_δ are the plasma density and velocity, respectively, at the freestream edge of the rotationally symmetric boundary layer formed on the anode surface. Hence in order to measure the velocity at a distance z from the cathode tip, an arc gap of $z + \delta$ is needed. The axial velocity owing to the cathode jet and the temperature outside the boundary layer are assumed to be independent of the arc gap. Temperatures at the edge of the anode boundary layer, needed to evaluate the plasma density, are taken from the measurements reported under Measurement of the Temperature Distribution.

Schoeck[7] calculates the boundary layer thickness at the anode stagnation point. His analysis shows that the boundary layer thickness is proportional to $\sqrt{\nu_\delta/(dV_s/dr)|_0}$ where ν_δ is the kinematic viscosity of the plasma at the freestream edge of the boundary layer and $(dV_s/dr)|_0$ is the gradient of the freestream velocity along the anode. surface evaluated at the stagnation point. Schoeck measures this gradient using a traversing pressure-tapped anode Because of the weak dependence of the boundary layer thickness on this velocity gradient and since it is difficult to perform these experiments with the fixed anode of this study, data at a given arc gap for $(dV_s/dr)|_0$ are extrapolated to 200 amp, the arc current selected in this study, from values reported by Schoeck at 50, 100, and 150 amp. The resulting boundary layer thicknesses and measured stagnation pressures are applied in a trial-and-error solution for the velocity. The values of velocity obtained with a sharply pointed cathode are summarized in Table 2.

The velocity in a plane perpendicular to the axis of the 10 mm arc at a point off the axis cannot be measured satisfactorily by a pressure-tapped anode. At all points, except the stagnation point, the velocity field caused by the cathode jet is altered by the presence of the anode. Other methods reported in the literature[5,6] for direct measurement of the entire velocity field also affect the velocity.

Therefore, an integration of the momentum equation for the flowing plasma is used to obtain values of the velocity relative to the velocity on the axis. In a plane perpendicular to the axis of the free-burning arc, the steady-state, non-viscous flow momentum equation and Maxwell's equations yield[4]:

$$p(r) - p(R) = \int_r^R j(\zeta)\,\frac{\mu_0}{\zeta}\left[\int_0^\zeta j(\tau)\tau\,d\tau\right]d\zeta \qquad (11)$$

where p is the pressure, j is the current density, and μ_0 is the permeability of vacuum. The coordinate r is the radial distance from the arc axis and R is the plasma radius in the plane of interest. Inserting the compressible, steady-state Bernoulli equation in eq (11), neglecting gravitational effects, and assuming that

Table 2—Cathode Jet Velocity from the Stagnation Pressure at the Anode of the 200 Amp Free-Burning Arc in Argon at 1 Atmosphere

Arc gap, mm	ΔP_o, dyne/cm²	δ, mm	$\rho_\delta \times 10^5$ (gm/cm³)	U, m/sec	Z at which U measured, mm
6.40	21,400	0.20	2.14	447	6.20
5.70	22,700	0.19	2.05	471	5.51
5.05	23,400	0.17	1.94	490	4.88
4.40	23,400	0.15	1.84	505	4.25
3.90	23,900	0.14	1.74	523	3.76
3.10	22,400	0.12	1.57	535	2.98
2.40	21,800	0.11	1.40	557	2.29
2.00	21,500	0.11	1.30	575	1.89
1.50	21,300	0.11	1.17	604	1.39
1.00	21,200	0.11	1.01	648	0.89

the flow is in the axial direction only leads to an expression for the flow velocity:

$$U(r) = \sqrt{2\int_r^R \frac{\mu_0 j(\zeta)}{\rho(\zeta)\zeta}\left[\int_0^\zeta j(\tau)\tau\, d\tau\right] d\tau} \quad (12)$$

where U is the cathode jet velocity and ρ the plasma density.

Ohm's Law, stated in eq (9), provides an expression for the variation of the current density in terms of the scalar electrical conductivity and the electric field intensity. The electrical conductivity is known as a function of temperature[12]. The electric field intensity near the flat anode can be assumed uniform[2]. Furthermore, the current density is subject to the condition:

$$I = 2\pi \int_0^R j(\zeta)\zeta\, d\zeta \quad (13)$$

where I is the total arc current, equal to 200 amp in this study. The velocity could, therefore, be calculated absolutely in planes where the assumption of a uniform electric field intensity is valid. However, in this method, the absolute current densities are subject to large errors owing to inaccurate knowledge of the plasma radius R in the planes of interest.

Moreover, near the pointed cathode, a plot of the necessary current lines compatible with the observed bell shape of the free-burning arc shows that the electric field intensity is not uniform. In the planes of interest, the streamlines of the potential flow combining a point source and a uniform velocity field correspond in shape to the current paths in a free-burning arc from a pointed cathode to a flat anode. The basis of this analogy is that both phenomena are described by Laplace's equation in geometrically similar situations. In the fluid flow case, the coordinates of the stagnation surface form a half-body and confine the flow to a cylindrically symmetric region inside this boundary. In the arc, the current is assumed to flow within the boundary defined by the points of 1% ionization.

Adapting the expression from potential flow theory[13] to the present case yields, for the electric field intensity,

$$E_z(r)/E_z(r=0) = \left[1 - \frac{h_z^2 z}{(z^2 + r^2)^{3/2}}\right] \quad (14)$$

where h_z is the radial distance at which 1% ionization occurs in a plane at a distance z from the cathode tip. The resulting values of E_z are presented for a radius of 5 mm in Table 3. Note that the approach of the electric field intensity to constant values for planes near the anode is reproduced in the model.

With the relative value of the electric field intensity provided by eq (13), eq (9) provides the radial variation in current density. This, in turn, allows the integration of the momentum equation to be carried out for the radial variation in the velocity. Tabular data are generated at 200 radial positions and the integrations are performed numerically with Simpson's method. Absolute values of velocity in each plane are obtained by normalizing the relative velocities to the measured centerline velocity. A crossplot of these data is shown in Fig. 6.

The shapes of the lines of equal velocity in this Fig. 6 agree with those of Fig. 7, presented by Wienecke[5], for a 200 amp arc across approximately a 50 mm gap in air. The values of velocity attained here near the cathode are, in general, 50% higher. This is not surprising since the carbon cathode of Wienecke's arc is unable to sustain a sharp tip. The numerical integration technique is applied using the temperature profiles of the free-burning arc of Kimura and Kanzawa[6]. The resulting velocity profiles agree within the limits estimated by these authors for their measured velocity profiles.

To assess the effect of cathode shape on the velocity field, data are gathered

Table 3—Variation of Electric Field Intensity in Planes of the 200 Amp, 10 mm Free-Burning Arc in Argon at 1 Atmosphere

mm from cathode	T_{arc}, °K	Degree of ionization	$E_z(5)/E_z(0)$
1.55	9,530	0.015	0.20
2.90	9,870	0.020	0.48
4.05	10,430	0.033	0.63
5.40	10,900	0.050	0.77

with the pressure-tapped anode during long-time operation of the arc. In Fig. 8, these data are compared to the data for a sharply pointed cathode. Comparison is also made to Schoeck's data which reflect average results obtained with long-time operation of a free-burning arc. The scatter of the data with the sharply pointed cathode indicates the excellent reproducibility of the flow field in a free-burning arc with a sharply pointed cathode. The deterioration of the cathode tip severely affects this reproducibility as indicated by the scattered data obtained during operation of the arc an hour after loss of the cathode tip.

The loss of the cathode tip also severely affects the value of the cathode jet velocity. According to eq (10), the velocity is proportional to the square root of the ratio $\Delta P_0/\rho_\delta$. To estimate the effect on the velocity, the effect of cathode deterioration on the temperature field is neglected. This assumes a constant plasma density at the freestream edge of the anode boundary layer for a particular arc gap. In this conservative estimate, loss of the cathode tip immediately reduces the cathode jet velocity by 20–25%. Long-time operation with continued cathode deterioration results in reductions of the order of 50%.

Despite the large flow velocities, the high kinematic viscosity of the plasma produces a laminar flow field in the free-burning arc of this study. Laminar convection heat fluxes are approximately proportional to the square root of the velocity. Compared to the heat flux with a sharply pointed cathode, a reduction of 30% in the maximum convection heat flux to the anode results from prolonged operation of the free-burning arc after loss of the cathode tip. Moreover, unbalanced Lorentz forces acting on the charged particles generate the velocity field. These forces are directly proportional to the product of the current density and the magnetic field arising from the current flow, both of which decrease with decreased constriction of the arc at the cathode. The reduction in velocity, is therefore, accompanied by a decrease of the same order of magnitude in the anode current

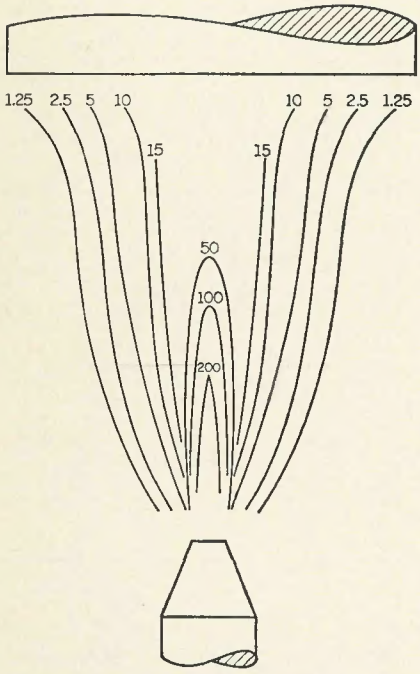

Fig. 7—Equal velocity curves of a 200 amp free-burning carbon arc

densities. Since the heat fluxes owing to the current flow are directly proportional to the current density[7], the reduction in electrical heat transfer is of the order of 50%.

Summary and Conclusions

Deterioration of the cathode tip of a gas-tungsten arc is a natural consequence of arc operation. To evaluate the influence of the cathode tip on the temperature and velocity fields in a gas-tungsten arc, a free-burning arc in argon at atmospheric pressure is studied in detail. The cathode configurations of gas-tungsten arcs and the free-burning arc used here are identical. It is shown that the free-burning arc with a sharply pointed cathode yields highly reproducible plasma conditions.

The temperature field obtained with a sharply pointed cathode is compared to that obtained from long-time operation of an identical arc. Slightly higher temperatures result near a sharply pointed cathode tip. Moreover, isotherms above 15,000° K are constricted to smaller radial distances from the arc axis and extend farther downstream from the cathode tip. A marked effect of cathode tip sharpness on the temperature field is not apparent however. It is speculated that the increase in temperature owing to the more severe constriction of the arc at the sharply pointed cathode is offset by increases in heat and mass transfer from the higher temperature regions. In the vicinity of the anode or, in the case of a gas-tungsten arc, at the workpiece, the effect of cathode tip sharpness on the temperature field is not significant.

The velocity field obtained with a

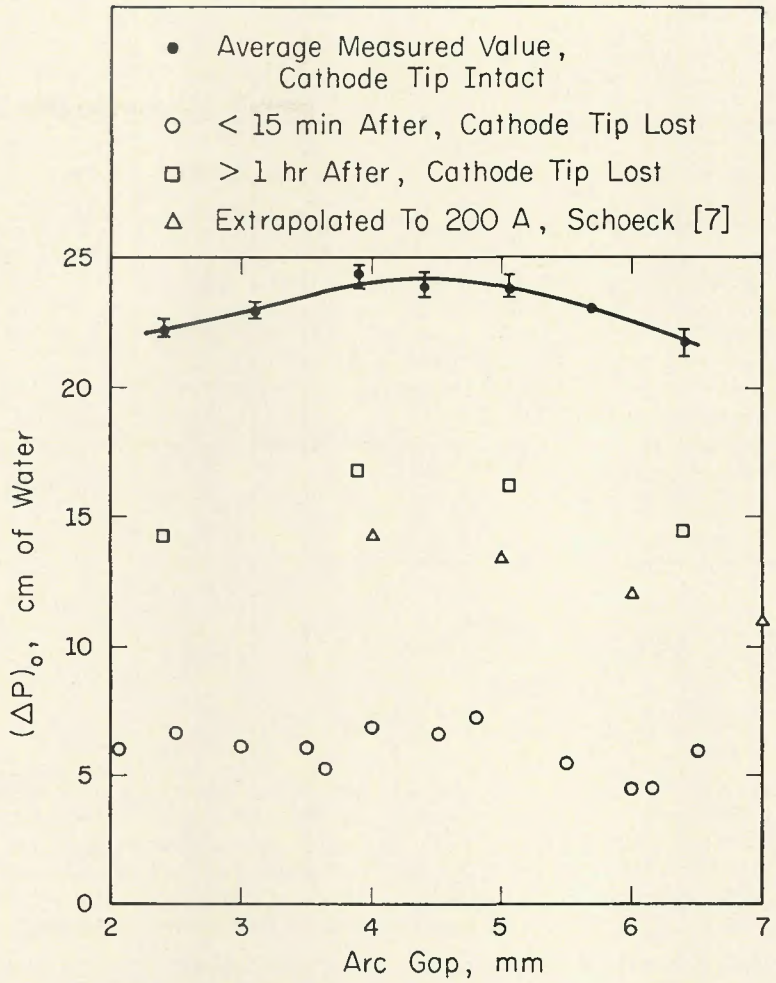

Fig. 8—Stagnation overpressure at the anode of a 200 amp free-burning arc in argon at atmospheric pressure

sharply pointed tungsten cathode is markedly different than the field obtained in an arc with a blunt carbon cathode at the same current level. The velocity is directly proportional to the product of the current density and the magnetic field arising from the current flow. The severe constriction of the arc at the sharply pointed tungsten tip leads to higher values of the current density and the magnetic field than in an arc with a blunt cathode. Direct comparison of the pressure at the stagnation point on the anode of a free-burning arc with and without a sharply pointed tungsten cathode confirms this conclusion. The flow velocity at the free-stream edge of the anode boundary layer is inferred from these measurements. The data show that a 50% reduction in velocity accompanies long-time operation of the free-burning arc with a blunt tungsten cathode.

The thermodynamic and transport properties of an argon plasma at atmospheric pressure vary with the temperature. Since the influence of the cathode tip on the temperature field is not felt near the anode, the values of plasma properties in the plasma near the anode are not changed. However, the increased constriction of the arc owing to a sharply pointed cathode significantly alters the heat flux distribution to the anode. The heat transfer due to the electrical current is directly proportional to the current density. The increase in current density accompanying increased constriction at a sharply pointed cathode is as much as 50%.

Since approximately half of the heat transfer to the anode is associated with the flow of charged particles to the anode[7], the peak heat flux at the center of the anode is increased by 25% owing to the increase in the current density. Moreover, an increase of 30% in the peak convective heat flux is associated with the 50% increase in the velocity on the axis of an arc with a sharply pointed cathode.

In a gas-tungsten arc, therefore, a sharply pointed cathode is expected to produce a deeper and narrower penetration of the workpiece. Furthermore, excellent reproducibility is evident in the data taken in this study to obtain the temperature and velocity fields. Thus, maintenance of a sharp cathode tip offers the possibility of more uniform quality of the weldments produced with

a gas-tungsten arc.

Acknowledgments

The results presented in this paper are part of a thesis submitted by T. W. Petrie to the faculty of the Graduate School of the University of Minnesota in partial fulfillment of the requirements for the degree of Doctor of Philosophy. Construction of and supplies for the apparatus used in this study were financed by the Welding Research Council of the AMERICAN WELDING SOCIETY and the National Science Foundation under Grant GK-1728. Free access to their digital computer facilities was granted by the University of Minnesota Computer Center. The authors gratefully acknowledge this assistance.

References

1. Olsen, H. N., "The Electric Arc as a Light Source for Quantitative Spectroscopy," *J.Q.R.S.T., 3,* 305-333 (1963).
2. Olsen H. N., "Thermal and Electrical Properties of an Argon Plasma," *Physics of Fluids, 2,* 614-623 (1959).
3. Wutzke, S. A., Cremers, C. J., and Eckert, E. R. G., "The Thermal Analysis of Anode and Cathode Regimes in an Electric Arc Column," University of Minnesota HTL TR 56 (1963).
4. Finkelnburg, W., and Maecker, H., "Elektrische Bögen und Thermisches Plasma," Handbuch der Physik, Bd. XXII, 254-444 (Springer-Verlag, Berlin, 1956). English translation, "Electric Arcs and Thermal Plasma," ARL 62-302 (1962).
5. Wienecke, R., "Über das Geschwindigkeitsfeld der Hochstromkohle bogensaüle," *Zeitschrift für Physik,* 143, 128-140 (1955).
6. Kimura, I., and Kanzawa, A., "Measurement of Stream Velocity in an Arc," *AIAA J., 1,* 310-314 (1963).
7. Schoeck, P. A., "An Investigation of the Energy Transfer to the Anode of High Intensity Arcs in Argon," Ph.D. Thesis, University of Minnesota (1961).
8. Cremers, C. J., and Birkebak, R. C., "Application of the Abel Integral Equation to Spectrographic Data," *Applied Optics, 5,* 1057-1064 (1966).
9. Olsen, H. N., "Measurement of Argon Transition Probabilities Using the Thermal Arc Plasma as a Radiation Source," *J.Q.R.S.T., 3,* 59-76 (1963).
10. Coates, P. B., and Gaydon, A. G., "Temperature Measurements in Shock Tubes; Transition Probabilities of Argon Lines," *Proc. Royal Soc., 293,* 452 (1966).
11. Evans, D. L., and Tankin, R. S., "Measurement of Emission and Absorption of Radiation by an Argon Plasma," *Physics of Fluids, 10,* 1137-1144 (1967).
12. DeVoto, R. S., "Transport Coefficients of Partially Ionized Argon," *Physics of Fluids, 10,* 354-364 (1967).
13. Streeter, V. L., *Fluid Dynamics* (McGraw-Hill, New York, 1948), Chap. IV.

USSR Welding Reasearch News

(*Continued from page* 587-s)

of the structural changes of the metal in the weld region due to the upset in the flash butt welding of steel parts. It was found that severe upsetting has a deleterious effect on the weld metal properties.

• Kakhovskii, N. T. et al.: Lowering of the carbon content in the weld metal in the manual welding of stainless steels (18-21).—It is shown that the introduction into the electrode coating of metal oxides with a melting point in excess of 2000° C makes it possible to obtain a substantial burnout of carbon from the welding rod. By introducing these oxides together with iron oxides, silicon may also be burned out.

• Yakobashvili, S. B.: Interphase tension of Armco iron at the boundary with ANF-1P flux (22-24).—Using the sessile drop method, the interphase tension at the separation boundary between a drop of liquid flux and the molten surface of Armco iron ($\sigma_{m\text{-}s}$) was measured. From the surface tension σ and from $\sigma_{m\text{-}s}$, the values for the cohesion, the adhesion and the coefficient of wetting were calculated. The surface tension and the density of the ANF-1P flux and the Armco iron were measured by the method of maximum gas bubble pressure.

• Kravchenko, E. L.: Cold welding of metals with a clean surface (25-27).—The results of a study of the cold welding of metals under vacuum are reported. The degree of deformation necessary for the cold welding of 24 pairs of dissimilar metals was determined. It is shown that the cold welding of metals is affected by the type and the crystal lattice of the metals, by their mutual solubility and by the ratio of their atomic diameters.

• Prokhorenko, V. M. and Zhdanov, I. M.: Brittle fracture of welded joints at room temperature (28-31).—The characteristics of welded joints at higher temperature are discussed and a two-stage mechanism for the growth of brittle-ductile cracks is suggested.

The energy relationships of this form of brittle fracture were analyzed.

• Demyanchuk, A. S. et al.: The chemical composition of the cut surface in the plasma arc cutting of metals (32-35).—The distribution of carbon acid of other alloying elements at the cut surface after the plasma arc cutting of metals has been studied.

• Lysov, V. S.: The static strength of a single row of resistance spot welds in AMg5M alloy (36-38).—The effect of the operating diameters and of the distance between the spots on the static strength of single rows of spot welds in AMg5M alloy 1.0 and 1.5 mm in thickness has been studied.

• Kasatkin, B. S. et al.: Welding of low-alloy high-strength 14Kh2GMR and 14KhMNDFR steel (39-42).—A welding procedure for these two grades of steel has been developed and recommendations are given for welding with coated electrodes, with the submerged arc and with the CO_2 shielded arc.

• Tsygan, B. G. et al.: Automatic welding of clad steel with metal powder addition (43-45).—Operating conditions for the automatic submerged arc welding of clad steels in two passes using metal powder additions have been worked out.

• Buchinskii, V. N. et al.: Pulsed arc overlay welding in argon with a powder wire (57-58).—An argon-shielded welding process with a powder electrode and its use for cladding the internal surface of a chemical reactor with a corrosion-resistant alloy is described.

• Shvartser, A. Ya. et al.: Electroslag surfacing and casting with a constant slag bath (60-63).—Electroslag surfacing and casting with the repeated use of the same slag bath have been studied. It was found that the consumption of flux is reduced significantly and the efficiency of the process is improved while the composition of the metal is changed only slightly.

• Veretnik, L. D. et al.: Removal of the risers of aluminum castings by plasma arc cutting (64-65).—The experimental use of plasma arc cutting for removing the risers of aluminum castings is described. It is shown that in order to improve the quality of the cuts it is necessary to change the location of the risers on the castings.

• Umanets, B. F.: Economic efficiency of pulsed arc welding with a consumable electrode (66-68).—The expediency and economic advantage of introducing pulsed arc welding with a consumable electrode in place of manual argon arc welding with a tungsten electrode in the fabrication with aluminum magnesium alloys has been demonstrated. An analysis of the relative cost of welding is also given.